

Experimental studies on mass transport in groundwater through fracture network using artificial fracture model

Takeo Tsuchihara¹, Masahito Yoshimura², Satoshi Ishida¹,
Masayuki Imaizumi¹, Ryouichi Ohonishi¹

¹National Institute for Rural Engineering, Tsukuba, Japan, ²DOWA Mining CO., Ltd., Tokyo, Japan

Abstract: A laboratory experiment using artificial fracture rocks was used to understand the 3-dimensional dispersion of a tracer and the mixing process in a fractured network. In this experiment, 12cm polystyrene foam cubes with two electrodes for monitoring electric conductivity (EC) were used as artificial fractured rocks. Distilled water with 0.5mS/m was used as a tracer in water with 35mS/m and the difference of EC between the tracer and the water was monitored by a multipoint simultaneous measurement system of electrical resistance. The results showed that even if the fracture arrangement pattern was not straight in the direction of the flow, the tracer did not diffuse along individual fractures and an oval tracer plume, which was the distribution of tracer concentrations, tended to be form in the direction of the flow. The vertical cross section of the tracer distribution showed small diffusivity in the vertical direction. The calculated total tracer volume passing through each measurement point in the horizontal cross section showed while that the solute passed through measurement points near the direction of hydraulic gradient and in other directions, the passed tracer volumes were small. Using Peclet number as a criterion, it was found that the mass distribution at the fracture intersection was controlled in the stage of transition between the complete mixing model and the streamline routing model.

1. Introduction

To solve new problems presented by the underground disposal of nuclear waste, bedrock underground storage, the use of underground space and so on, it is extremely important to obtain the information about the groundwater movement and the characteristics of diffusion of the solute in the fractured rock. The movement of groundwater in the fracture, which is the main passage in rocks, has been researched. The flow in the fractured rock depends on the geometrical characteristic of fractures; the scale, the distribution and the pattern of fractures, but it is difficult to obtain such information accurately for analysis. Especially in the analysis of a large-scale model such as the field investigations, the fractured rock has been considered as the equilibrium porous media in a lot of analyses. However, in order to do so, it is necessary to meet such conditions as the good connection of each fracture, the equal distribution of fractures and the randomness of their directions (Long et al., 1982).

On the other hand, the models that consider the fracture in rocks have been developed, but enormous data is necessary to use these models for the analysis. Moreover, there are two models; the complete mixing model and the streamline routing model, which simulate the dispersion mechanism at the fracture intersection, which is important factor in the movement of the solute. TRACR3D (Travis, 1984), FRAC3DVS(Suidicky, 1985, Therrien, 1996) assume the complete mixing at the intersection. However, it has been found that the complete mixing model was not necessarily applicable from the result of the experiment at the local fracture intersection, and a lot of numerical analyses have revealed that the streamline routing model could not explain this dispersion mechanism enough (Hull et al., 1987). In this research, a laboratory experiment using artificial fractured rocks confirmed the difference of hydraulic characteristics by three-dimensional fracture patterns, and accumulated the basic data for the elucidation of dispersion mechanism in the fracture network.

2. Experiment Method

Experimental Model

A laboratory experiment using artificial fracture networks was used to understand the effects of hydraulic factors in fractured rocks, that is, the direction and arrangement of fractures. In this experiment, polystyrene foam blocks that were 12 cm cubes were used as base rocks. The artificial fractured rocks were comprised of these blocks, and 360 blocks were combined into a three-dimensional space with fracture. The fracture aperture was 0.8 mm and the dimensions of the experimental fractured rock were 0.72 m×1.2 m×0.72 m. The experimental fractured rock

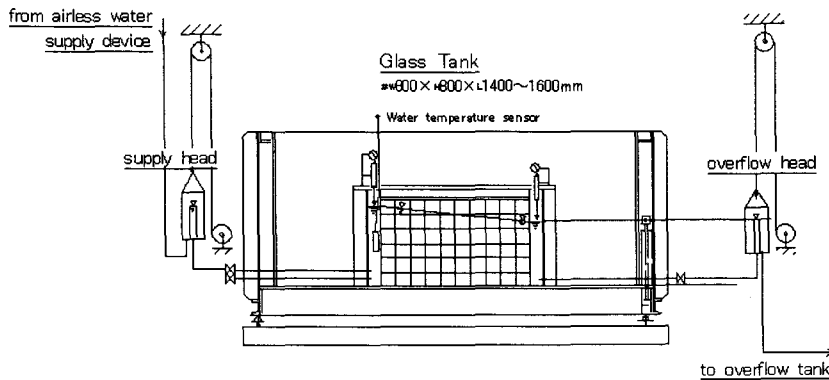


Fig. 1. Overview of the experiment system.

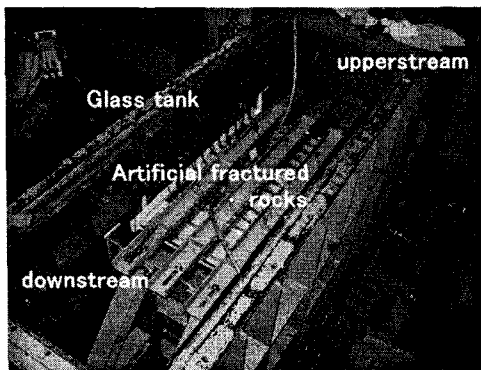


Fig. 2. Experiment system set-up.

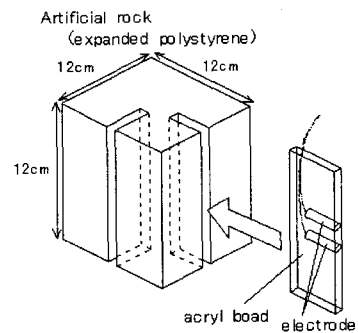


Fig. 3. Artificial rock and setting of electrodes.

combination was placed in a glass water tank, and the side and the base were fixed on the glass tank with a water-resistant adhesive. An acrylic board was set on the upper side of the fractured rock and given a load to prevent the floating of the polystyrene foam blocks.

Fig.1 shows an overview of this experiment system and Fig.2 shows a picture of its set-up. The tracer was instantaneously injected by a syringe through a vinyl tube inserted beforehand. In this experiment, the fracture aperture was so small that the airless water that was made by a suction of a vacuum pump was used to prevent the generation of air bubbles in fractures.

Electric Conductivity Measurement

In this experiment, the electric conductivity was measured to detect changes in tracer concentrations. In order to measure the electric conductivity, electrodes were installed in artificial base blocks. The electrodes were made of stainless steel with a diameter of 2 millimeters and buried in polystyrene foam blocks while the part used for measurement was left on the block surface. The electrodes and electric wires were covered by acrylic boards to keep them away from the water. A total of 96 electrodes was set up. Fig.3 shows the polystyrene foam block and the arrangement of electrodes. For the measurement using these electrodes, an alternating current (AC) power was used to prevent polarization, and the resistance of water transformed from a voltage ratio between two electrodes of each measurement point was converted into the electric conductivity. In this experiment, the distilled water was used as the tracer to take advantage of the differences of electric conductivities between distilled water and tap water. The electric conductivity of the tap water used in this experiment was about 35 mS/m, while that of the distilled water was about 0.5 mS/m; about a 70 times difference. An other merit adopting distilled water as a tracer that the effect from the difference of density between water and tracer was negligible. Each electrode set had a different contact area with the water and different distance between two electrodes; therefore, the relationships between the resistance and electric conductivity were identified beforehand by pouring some water with different already-known

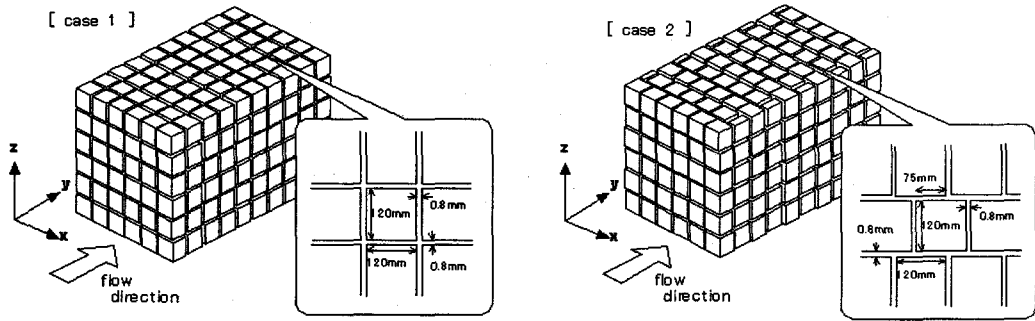


Fig. 4. Fracture pattern of artificial fractured blocks (case 1 and case 2).

electric conductivities and measuring them in all electrode sets. Generally, the electric conductivity is in inverse proportion to the resistance of the water.

Electric conductivity C is converted into the relative electric conductivity C_r in the following equation,

$$C_r = \frac{C_b - C}{C_b - C_t} \quad (1)$$

where C is the electric conductivity at the measurement point, C_b is the electric conductivity of the tap water, and C_t is electric conductivity of the tracer (distilled water). C_r has a range from 0 to 1.

Fracture Pattern

Fig.4 shows the arrangement of artificial fractured rocks and fracture patterns. The direction of flowing is the y -axis, the horizontal direction is the x -axis and the vertical direction is the z -axis. The fracture pattern in case 1 has straight-line fractures in the x , y and z -directions and all fracture apertures are 0.8mm. The fracture pattern in case 2 has the same fracture apertures, but each fracture row in the y -direction is moved by 45 mm or 75mm, and a winding fracture pattern was formed.

Dispersion coefficient

A basic transport model, which can be used for analysis in these experiments, is the one-dimensional advection-dispersion model. In this research, this model was adopted to estimate the dispersion coefficient. The equation is written as,

$$D \frac{\partial^2 C}{\partial x^2} - v \frac{\partial C}{\partial x} = \frac{\partial C}{\partial t} \quad (2)$$

where D is the longitudinal dispersion coefficient in the direction of flow x , C is concentration and v is the mean fluid velocity. The following initial condition is applied, and the solution (equation (6)) can be obtained using Laplace transform method. (Kinzelbach, 1990 and Raven et al., 1988)

$$C(x,0) = 0 \quad (3)$$

$$-D_L \frac{\partial C}{\partial x}(0,t) + vC(0,t) = M\delta(x) \quad (4)$$

$$C(+\infty, t) = 0 \quad (5)$$

$$C(x,t) = \frac{M}{(\pi D_L t)^{1/2}} \exp\left\{-\frac{(x-vt)^2}{4D_L t}\right\} - M \left[\frac{v}{2D_L}\right] \exp\left\{\frac{vx}{D_L}\right\} \operatorname{erfc}\left[\frac{(x+vt)}{2(D_L t)^{1/2}}\right] \quad (6)$$

where D_L is the longitudinal dispersion coefficient, M is the mass of tracer per unit and erfc is the complementary error function. In this experiment, the tracer was instantaneously injected as a pulse, which expressed the Dirac impulse function $\delta(x-x')$ where $x'=0$, multiplied by M . The fluid velocity is assumed to be large enough not to undergo the opposite-direction flux by the tracer injection, and the tracer and the water that originally existed at the injection point are assumed to be completely mixed at the time of the injection.

Reynolds number

Reynolds number (Re) is a dimensionless number that expresses the ratio of inertial to viscous forces and is used as the index of the transition from laminar to turbulent flow. Re is written as,

$$Re = \frac{v \cdot l}{\nu} \quad (7)$$

where v is the mean fluid velocity, l is the diameter of the pipe and ν is the dynamic viscosity. Generally, l is replaced by the effective diameter of the grain in porous media and by the hydraulic radius or the mean depth in open channels. However, it is doubtful whether the fracture aperture can be assumed to be l in the case of fractured rock. In fractured rocks, it is difficult to determine the Reynolds number, since the flow varies greatly from one point to another along the same fracture. Sato (1984) expressed the following equation,

$$Re = \frac{v \cdot \sigma}{\nu} \quad (8)$$

where σ is representative length, which is defined as the radius of pipe equivalent to total pore volume. Marsily (1986) represented the following equation using D_h in the fracture that consists of parallel boards,

$$Re = \frac{v \cdot D_h}{\nu}, \quad D_h = \frac{4A}{p} \quad (9)$$

where A is cross-sectional area, which is shown as $A=Hb$, p is outer length of cross-section, which is shown as $p=2(H+b)$, H is fracture width, b is fracture aperture. If $H \gg b$, the Reynolds number is approximated as,

$$Re \approx \frac{2Q}{\nu H} \quad (10)$$

where Q is flow rate passing through fracture. Yoshimura (2002) experimentally showed the linear relation between the both Reynolds number by Sato (1984) and Marsily (1986). In this research, Reynolds number was calculated using the Sato's equation.

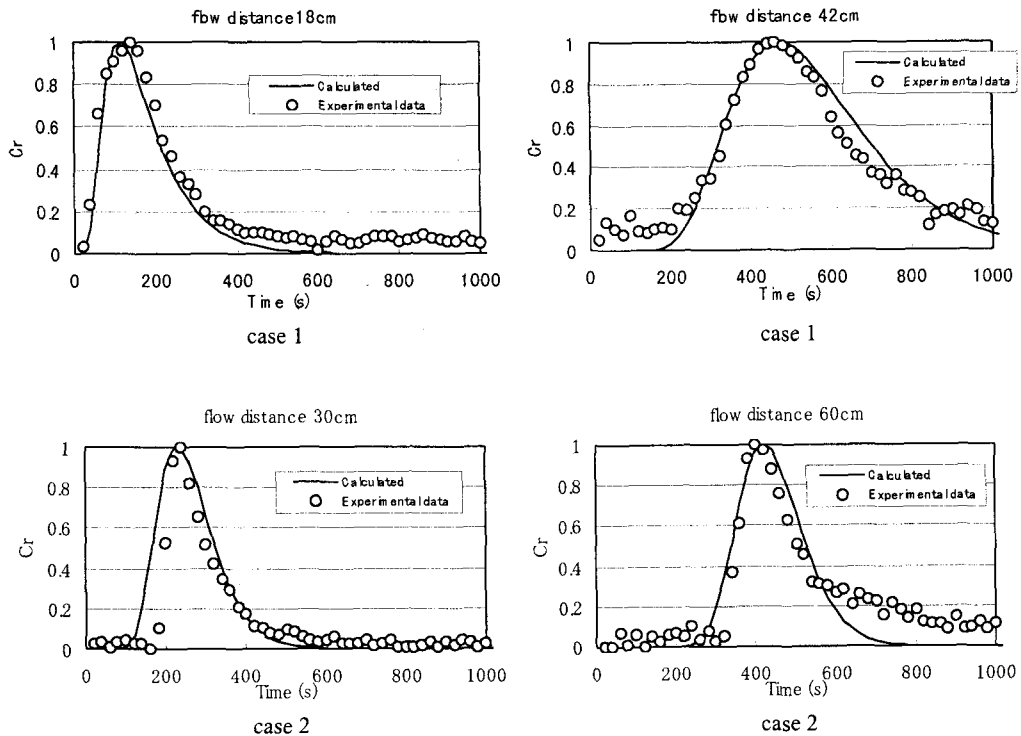


Fig. 5. Comparison of tracer concentration between experimental data and analytical solution of one-dimensional advection dispersion equation in case 1 (flow distance=30, 60cm) and case 2 (flow distance=18, 42cm).

Table 1. Hydraulic parameters in experiments.

	i	v (m/s)	K (m/s)	n^*	Re	α_L (m)	α_T (m)
case 1	0.00124	2.08×10^{-3}	1.68	1.46 %	1.24×10^2	2.50×10^{-2}	1.25×10^{-2}
case 2	0.00124	1.44×10^{-3}	1.16	2.17 %	8.58×10^1	6.25×10^{-3}	6.67×10^{-3}

*Porosity n in case 1 is the porosity that has influence on the flow, in which orthogonal fractures for hydraulic gradient are excluded.

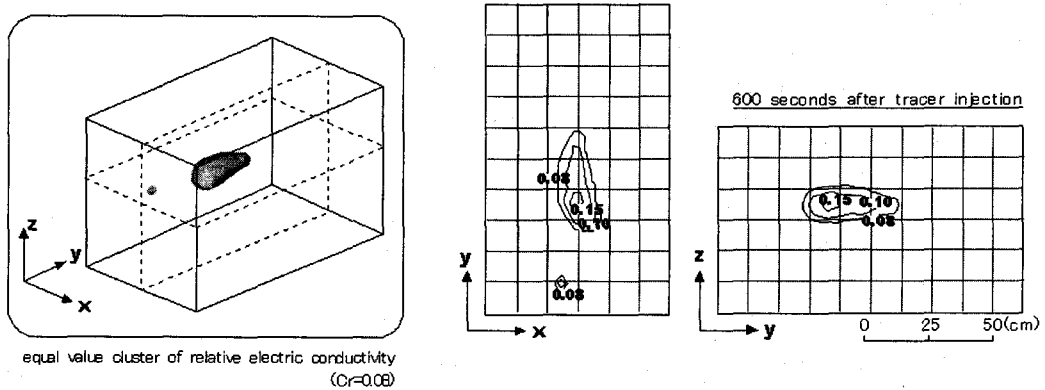


Fig. 6. Tracer distribution in experiment case 1 (600 seconds after tracer injection).

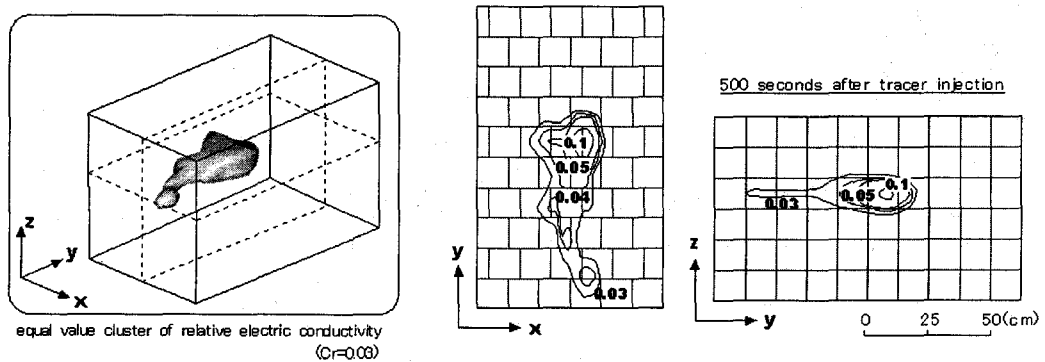


Fig. 7. Tracer distribution in experiment case 2 (500 seconds after tracer injection).

3. Results

The hydraulic parameters in experiments are shown in Table 1. Reynolds number was 1.24×10^2 in case 1 and 8.58×10^1 in case 2. Reynolds number was enough small in both cases to conclude that the flow in the fracture network was laminar flow. Thus, hydraulic conductivity coefficients were calculated assuming that Darcy's law was applicable. Longitudinal dispersivity and transverse dispersivity was obtained by comparing tracer concentrations between experimental data and analytical solution of one-dimensional advection-dispersion equation. Fig. 5 shows examples of these comparisons.

It was necessary to display the distribution of tracer concentration in the fracture because the solute transportation in this experiment only occurred in fractures. However, to make the situation of the solute transportation with each case with a different fracture pattern visible, the tracer concentration was distributed based on the electric conductivity data that had been obtained at each measurement point. This distribution contour to define a certain concentration is called a plume.

Fig.6 and Fig.7 show typical experimental results. The same tendency was shown in other hydraulic gradient case. Fig.6 shows the distribution plume of tracer concentration at 600 seconds after the tracer injection in case 1. The three-dimensional plume is equal-value cluster of the relative electric conductivity, $C_r=0.08$ and the two-dimensional plumes are xy - and yz -cross sections. As this figure shows, an oval tracer plume was formed in the direction of the flow and there was small diffusion in both horizontal and vertical directions. Fig.7 shows the distribution plume of tracer concentration at 500 seconds after the tracer injection in case 2. The fracture pattern in case winds in the y -direction, which differs from the pattern in case 1, however, the tracer plume was formed in the flow direction without each fracture diffusing. The yz -cross section shows that the diffusivity in the vertical direction was also small. From experimental results, the solute in fracture network was expected to move along streamlines with little mixing and distribution in fracture intersection parts.

In order to verify what route the tracer took, the total amount of tracer passing through each measurement point was obtained as an integrated value of the electric conductivity. Fig.8 shows the ratio to the total amount of tracer in the xy -cross section. In this figure, the ratio is represented as a bar chart in each line along horizontal direction. As this figure indicates, the tracer passed in the direction of the hydraulic gradient at a high rate, and was not distributed evenly at fracture intersections. However, the movement of solute was not completely controlled by streamline.

The complete mixing model and the streamline routing model have been proposed by many researchers to explain the movement of solute at fracture intersections. The complete mixing model assumes that the solute is completely mixed and re-distributed at fracture intersections (Krizek et al., 1972, Schwartz et al., 1983, Smith and Schwartz, 1984, Schwartz et al., 1988). On the other hand, the streamline routing model assumes that the solute moves along the streamline without mixing at fracture intersections (Wilson and Witherspoon, 1976, Endo et al., 1984, Hull et al., 1987, Philip, 1988, Park and Lee, 1999). Peclet number (Pe) is also related to the movement of the solute in a fracture. When Peclet number is large, the streamline routing model is effective, but when it is small, the results of numerical computing come close to the complete mixing model (Berkowitz et al., 1994, Park and Lee 1999). However, in the case of a small Peclet number, the influence of boundary conditions and flowing length becomes large and cannot be negligible. In $Pe \gg 1$, the complete mixing model is applicable and in $Pe \ll 1$, the streamline routing model is applicable. However, it should be noted that the flow of real fracture networks is caused within the middle range of Peclet numbers (Mourzenko et al., 2002).

Berkowitz et al. (1994) defined Peclet number as follows,

$$Pe = \frac{vr}{D} \quad (12)$$

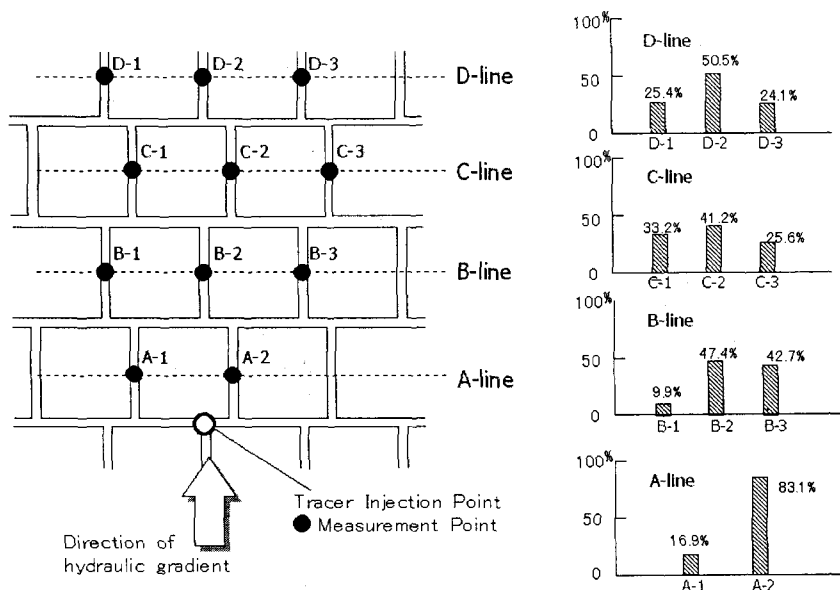


Fig. 8. Ratio to total amount of tracer passing through fracture network in xy -cross section.

where v is mean velocity, D is dispersion coefficient and r is a representative length, which corresponds to the distance across a fracture intersection. According to this equation, the Peclet number was 0.118 in case 1 and 0.109 in case 2. Fig.9 show a comparison of mixing characteristics at fracture intersection that was drawn by Park and Lee (1999) with our experiment result. As this figure shows, the movement of the solute at the fracture intersection was in a transition zone between the complete mixing model and the streamline routing model. Although there have been various attempts to model the solute in the fracture intersections, there are few examples of experimental verification. With the development of numerical modeling, experimental verification will be necessary especially for large-scale models near field research in the future.

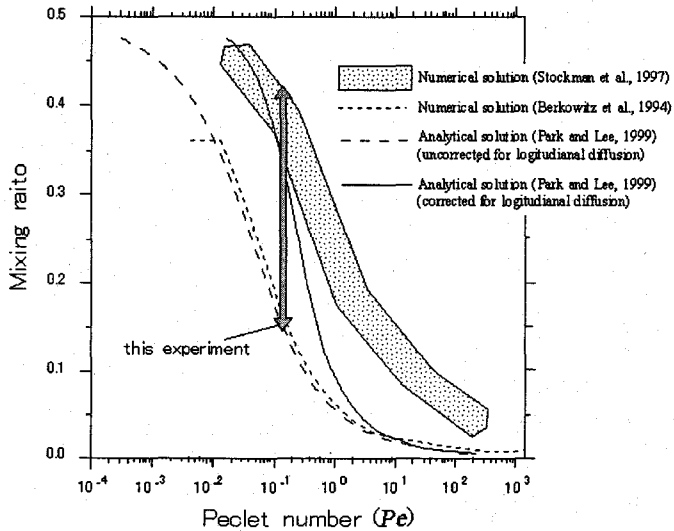


Fig. 9. Comparison of mixing characteristics at fracture intersection (modified from Park and Lee, 1999).

4. Conclusions

Tracer experiments in three-dimensional fracture network using artificial fractured rock revealed that the solute flowed mainly in the direction of the hydraulic gradient regardless of the fracture pattern arrangement, and dispersions in both the horizontal and the vertical directions were small. In addition, by obtaining the total volume of the tracer passing through each measurement point, it was found that the solute was not completely mixed and was re-distributed at each fracture intersection. However, the movement of solute was not completely controlled by streamline in this experiment. Using Peclet number, which is the ratio of advection to dispersion, as a criterion, it was found that the mass distribution at a fracture intersection was controlled in the stage of transition between the complete mixing model and the streamline routing model. Thus, it was experimentally confirmed that Peclet number was an effective index for understanding the flow condition in a fracture network.

The contribution of fundamental data obtained by laboratory experiments is also large, since in the case of field researches, data are difficult to collect, and are often unreliable, and too complex to interpret. The further accumulation of experiment data especially in the large-scale model near field conditions is necessary.

References

Berkowitz, B., Naumann, C., Smith, L., 1994, Mass transfer at fracture intersections: An evaluation of mixing models, *Water Resources Research*, Vol.30, No.6, 1765-1773.
 Endo, H. K., Long, J. C. S., Wilson, C. R., Witherspoon, P. A., 1984, A Model for Investigating Mechanical Transport in Fracture Networks, *Water Resources Research*, Vol.20, No.10, 1390-1400.
 Hull, L.C., Koslow, K. N., 1986, Streamline Routing Through Fracture Junctions, *Water Resources Research*, Vol.22, No.12, 1731-1734.

- Kinzelbach, W., 1990, Groundwater modeling, Morikita Shuppan, Tokyo, p.286. [in Japanese]
- Krizek, R. J., Karadi, G. M., Socias, E., 1972, Dispersion of a contaminant in fissured rock, paper presented at Symposium on percolation Through Fissured Rock, Int. Soc. of Rock Mech., Stuttgart, Germany.
- Long, J. C. S., Remer, J. S., Wilson, C. R., Witherspoon, P. A., 1982, Porous Media Equivalents for Networks of Discontinuous Fractures, *Water Resources Research*, Vol.18, 645-658.
- Marsily, G. de, 1986, *Quantitative Hydrogeology*, Academic Press, New York, p.440.
- Mourzenko, V. V., Yousefian, F., Kolbah, B., Thovert, J.-F. and Alder, P. M., 2002, Solute transport at fracture intersections, *Water Resources Research*, Vol.38, No.1, 1.1-1.14.
- Park, Y. J., Lee, K. K., 1999, Analytical solutions for solute transfer characteristics at continuous fracture junctions, *Water Resources Research*, Vol.35, No.5, 1531-1537.
- Philip, J. R. (1988): The Field Mechanics of Fracture and Other Junctions, *Water Resources Research*, 24(2), pp.239-246
- Raven, K. G., K. S. Novakowski, Lapcevic, P. A., 1988, Interpretation of Field Tracer Tests of a Single Fracture Using a Transient Solute Storage Model, *Water Resource Research*, Vol.24, No.12, 2019-2032.
- Sato, K., Sasaki, Y., 1984, Experimental Determination of Solute Dispersion Coefficients in Rock Seepage, *Journal of the Japan Society of Engineering Geology*, Vol.25, No.3, 3-10. [in Japanese]
- Schwartz, F. W., Smith, L., Crowe, A. S., 1983, A Stochastic Analysis of Macroscopic Dispersion in Fractured Media, *Water Resources Research*, Vol.19, No.5, 1253-1265.
- Schwartz, F. W., Smith, L., 1988, A Continuum Approach for Modeling Mass Transport in Fractured Media, *Water Resources Research*, Vol.24, No.8, 1360-1372.
- Smith, L., Schwartz, F. W., 1984, An Analysis of the Influence of Fracture Geometry on Mass Transport in Fractured Media, *Water Resources Research*, Vol.20, No.9, 1241-1252.
- Suidicky, E. A., Unger, A. J. A., Lacombe, S., 1995, Three-dimensional analysis technique for the direct implementation of well bore boundary conditions in three-dimensional heterogeneous formations, *Water Resources Research*, Vol.31, No.2, 411-415.
- Therrien, R., Suidicky, E. A., 1996, Three-dimensional analysis of variably-saturated flow and solute transport in discretely-fractured porous media, *Journal of Contaminant Hydrology*, Vol.23, No.1,2, 1-44.
- Wilson, C. R., Witherspoon, P. A., 1976, Flow Interference Effects at Fracture Intersections, *Water Resources Research*, Vol.12, No.1, 102-104.
- Yoshimura, M., 2002, Studies on Groundwater Flow and Solute Transport in Rocks, Doctoral Thesis, Chiba University, p.77. [in Japanese]